Title

Human stem cell—derived astrocytes replicate human prions in a PRNP genotype—dependent manner

Permalink

https://escholarship.org/uc/item/6wd40042

Journal

Journal of Experimental Medicine, 214(12)

ISSN

0022-1007

Authors

Krejciova, Zuzana
Alibhai, James
Zhao, Chen
et al.

Publication Date

2017-12-04

DOI

10.1084/jem.20161547

Peer reviewed

Human stem cell–derived astrocytes replicate human prions in a *PRNP* genotype–dependent manner

Zuzana Krejciova,[1,7]* James Alibhai,[1]* Chen Zhao,[2] Robert Krencik,[9] Nina M. Rzechorzek,[2,3] Erik M. Ullian,[8] Jean Manson,[4] James W. Ironside,[1] Mark W. Head,[1] and Siddharthan Chandran[2,5,6,10]

[1]National CJD Research & Surveillance Unit, Centre for Clinical Brain Sciences, [2]Medical Research Council Centre for Regenerative Medicine, [3]Royal (Dick) School of Veterinary Studies and The Roslin Institute, [4]Neurobiology Division, The Roslin Institute, [5]UK Dementia Research Institute, and [6]Centre for Clinical Brain Sciences, University of Edinburgh, Edinburgh, Scotland, UK
[7]Institute for Neurodegenerative Diseases and [8]Department of Ophthalmology, University of California, San Francisco, San Francisco, CA
[9]Department of Neurosurgery, Center for Neuroregeneration, Houston Methodist Research Institute, Houston, TX
[10]Centre for Brain Development and Repair, Institute for Stem Cell Biology and Regenerative Medicine, National Centre for Biological Sciences, Bangalore, India

Prions are infectious agents that cause neurodegenerative diseases such as Creutzfeldt–Jakob disease (CJD). The absence of a human cell culture model that replicates human prions has hampered prion disease research for decades. In this paper, we show that astrocytes derived from human induced pluripotent stem cells (iPSCs) support the replication of prions from brain samples of CJD patients. For experimental exposure of astrocytes to variant CJD (vCJD), the kinetics of prion replication occur in a prion protein codon 129 genotype–dependent manner, reflecting the genotype-dependent susceptibility to clinical vCJD found in patients. Furthermore, iPSC–derived astrocytes can replicate prions associated with the major sporadic CJD strains found in human patients. Lastly, we demonstrate the subpassage of prions from infected to naive astrocyte cultures, indicating the generation of prion infectivity in vitro. Our study addresses a long-standing gap in the repertoire of human prion disease research, providing a new in vitro system for accelerated mechanistic studies and drug discovery.

INTRODUCTION

Prions are protein-based transmissible pathogens responsible for fatal neurodegenerative diseases of the central nervous system (CNS), such as Creutzfeldt–Jakob disease (CJD; Prusiner, 2013). CJD can be sporadic (sCJD), genetic, iatrogenic (iCJD), or zoonotic (such as variant CJD [vCJD]) and is uniformly untreatable, presenting a significant public health concern. The CJD prion is a misfolded and aggregated conformer of the host-encoded prion protein (PrP) that replicates by seeded self-propagating conversion of the host's normal cellular prion protein (PrP^C) to the disease-associated scrapie form (PrP^{Sc}). The genotype at the polymorphic codon 129 of the human prion protein gene (*PRNP*), methionine/methionine (MM), methionine/valine (MV), and valine/valine (VV), is critical in determining disease susceptibility and, in combination with the conformer of PrP^{Sc} present (type 1 or type 2), defines the disease phenotype. For example, all but one of the 178 definite clinical cases of vCJD worldwide have occurred in individuals homozygous for methionine at codon 129 of *PRNP* (Mok et al., 2017), whereas sCJD occurs in all three codon 129 genotypes with distinct phenotypic sub-

types, such as the common MM1 and VV2 subtypes of sCJD (Parchi et al., 1999, 2009).

The mechanisms underlying susceptibility, including cell type specificity, to infection and the sequence of events that lead to neurodegeneration in CJD are poorly understood. Although infectious prions can accumulate in a range of tissues and organs expressing PrP^C, the pathological effects of prion replication appear to be restricted to a progressive neurodegenerative cascade in the CNS, which can be extrapolated from animal models of prion diseases (Cunningham et al., 2003; Gray et al., 2009; Alibhai et al., 2016). Notwithstanding the importance of small and large animal models to our understanding of the pathobiology of prion diseases, there is an urgent need for complementary experimental systems to model aspects of human prion diseases (Jones et al., 2011; McCutcheon et al., 2011; Watts and Prusiner, 2014). In this regard, cell-free assays have provided important insights into prion composition, prion strains, and barriers to prion transmission (Wang et al., 2010; Deleault et al., 2012; Krejciova et al., 2014a). Against this background, the availability of a scalable and physiologically relevant human-based cellular experimental system to study human prion diseases—including the modeling of neuronal–glial interactions that are increasingly thought to be involved in neurodegenerative diseases—would be of great value (Gómez-Nicola et al., 2013; Asuni et al.,

2014; Hennessy et al., 2015; Liddelow et al., 2017). However, to date, no human cell lines have been described that are directly and reproducibly susceptible to infection with human prions from a CJD brain. The literature contains only one, as yet unconfirmed, study of direct sCJD prion infection of a human immortalized SH-SY5Y neuroblastoma cell line (Ladogana et al., 1995). Consequently, the majority of cell biology studies of prion replication and its inhibition continue to be performed using mouse-adapted prion strains in transformed or transgenic rodent cells (Grassmann et al., 2013). Rodent-adapted CJD prions have been shown to replicate in an immortalized hypothalamic GT-1 cell line (Arjona et al., 2004) and rabbit epithelial cell line RK13 expressing mouse PrP (Lawson et al., 2008). vCJD and sCJD prions have also been shown to replicate in cerebellar granule cells from transgenic mice overexpressing human PrP (Cronier et al., 2007; Hannaoui et al., 2014). Each of these examples involved the passage of human prions through intermediate species and/or the use of recipient cells with an experimentally modified *PRNP* genotype, arguably diminishing the relevance of these culture models to the study of human prion mechanisms of disease. The inadequacy of current cell culture models of human prion disease likely contributes to the translational failure of apparently promising antiprion compounds from the laboratory to clinical practice (Trevitt and Collinge, 2006; Stewart et al., 2008; Berry et al., 2013; Watts and Prusiner, 2014; Giles et al., 2015).

In this study, we establish the first human cell culture model that can replicate human prions directly from CJD-affected brain tissue. We hypothesize that the prerequisites for human prion replication in vitro would include matching of agent (inoculum) and host (cell) PrP sequences (specifically, the critical M/V polymorphism at codon 129 of *PRNP*) and a relevant differentiated human CNS cell type. We tested these requirements for prion infection by exposing astrocytes derived from human induced pluripotent stem cells (iPSCs) of defined codon 129 genotypes to human prions from vCJD and sCJD brains.

RESULTS AND DISCUSSION
Characterization of human iPSC–derived astrocyte progenitor cells (APCs) and astrocyte cultures
Astrocytes were generated from iPSC lines using a previously established protocol (Fig. 1 A; Krencik and Zhang, 2011; Serio et al., 2013). All iPSC lines used in this study have been previously demonstrated to generate functional and highly enriched (>90%) astrocyte populations (Krencik and Zhang, 2011; Serio et al., 2013; Krencik et al., 2015). After *PRNP* genotyping, two MM (iPSC1 and iPSC4), one MV (iPSC2), and one VV (iPSC3) cell line were selected for the generation of APCs and astrocytes. Quantitative immunocytochemistry of epidermal growth factor (EGF)/fibroblast growth factor (FGF)–treated cultures revealed a highly enriched APC-containing population defined by expression of APC markers vimentin (iPSC1, 97.1 ± 1.2%; iPSC2, 90 ±

0.6%; iPSC3, 98.5 ± 0.2%) and nestin (iPSC1, 98.2 ± 2.2%; iPSC2, 99.1 ± 0.5%; iPSC3, 98.7 ± 0.3%; Fig. 1 B). After the withdrawal of mitogens and addition of ciliary neurotrophic factor (CNTF), astrocyte cultures expressing extracellular L-glutamate/L-aspartate transporter (GLAST; Fig. 1 C) and GFAP⁺ (iPSC1, 87.8 ± 1.7%; iPSC2, 91.4 ± 1.7%; iPSC3, 89.2 ± 0.7%) were generated with comparably low levels of other CNS cell markers present, such as NeuN (neurons), O4 and Olig2 (oligodendrocytes), and Iba1 and CD68 (macrophages; Fig. 1 D and Fig. S1). Comparable differentiation efficiency was observed across all iPSC lines. Immunolabeling for the cell proliferation marker Ki67 showed significantly reduced proliferation of differentiated astrocyte cultures compared with APC cultures (Fig. 1 E). Functional evaluation of iPSC-derived APC and astrocyte cultures confirmed differentiation-dependent (astrocyte) functional up-regulation of the ability to take up extracellular L-glutamate in a time-dependent manner with no differences between lines (Fig. 1 F). Having established enriched astrocyte populations, we next confirmed expression of PrP^C across all genotypes (Fig. 1 G). Immunocytochemistry suggests that PrP^C resides predominantly on the cell surface, which is consistent with the known localization of PrP^C in cultured cells (Fig. 1 H; Stahl et al., 1987).

CJD brain samples of different *PRNP* genotypes (Fig. 1 I) used to infect cells were prepared by homogenization, sonication, and filtration to produce a clarified and well-dispersed inoculum with a predefined upper limit to particulate size. To determine whether brain homogenate–derived inocula are toxic to astrocytes, we measured cell viability immediately and at 3 d after 24-h exposure of 1% vCJD, 1% sCJD, or control normal brain homogenate (NBH) inoculum. Cell viability was >95% with no difference between exposed and unexposed control cells at either time point across all genotypes (Fig. 1 J).

Astrocytes are susceptible to direct infection with human prions in a *PRNP* codon 129–dependent manner
Because APC cultures express PrP^C, we performed preliminary experiments to assess the ability of these highly proliferating cells to propagate and accumulate CJD prions after 24-h exposure to 1% vCJD or sCJD brain homogenates. APC cultures were analyzed for PrP^{Sc} accumulation at 0, 3, and 8 d post exposure (dpe). All APC cultures, regardless of genotype, showed a loss of detectable levels of protease-resistant PrP^{Sc} in cultures up to 8 dpe to vCJD homogenate (Fig. 2, A and B) or two different types of genotype-matched sCJD, VV1 or VV2 (Fig. 2, C and D). This indicated that proliferating precursor cells are refractory to prion propagation, which is consistent with our previous results (Krejciova et al., 2011).

We next evaluated the capacity of CNTF-differentiated, predominantly postmitotic astrocyte cultures to propagate human prion strains. MM, MV, or VV genotype astrocytes were first tested for their ability to support prion replication using vCJD brain homogenate (Fig. 2, E–G). Noting that
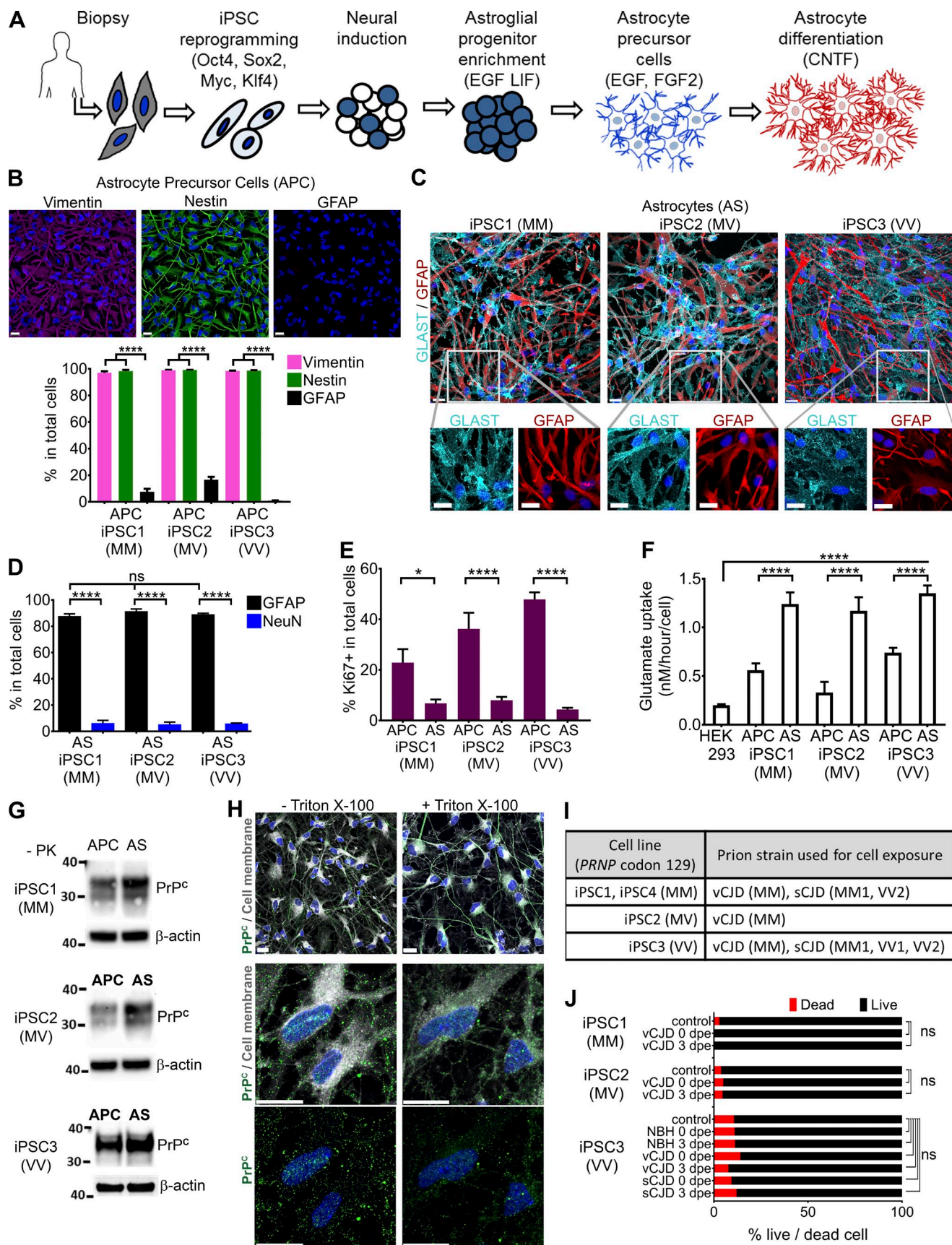
all vCJD cases with one exception have occurred in MM individuals, we hypothesized a greater susceptibility of MM astrocytes to vCJD (MM) exposure. Immunoblot analysis for protease-resistant PrP^{Sc} at 3 and 8 dpe in MM astrocytes revealed significant accumulation of PrP^{Sc} that substantially exceeded the amount of PrP^{Sc} in the initial vCJD inoculum, as determined by linear regression analysis (Fig. 2 E). In contrast, MV and VV astrocytes failed to replicate vCJD (MM) prions to detectable levels at the same time points (Fig. 2, F and G). To test whether VV astrocytes that failed to replicate vCJD (MM) prions were capable of replicating prions with a matched genotype, we next exposed VV astrocytes to sCJD homogenate derived from a patient homozygous for valine at codon 129 (VV2 subtype). Quantitative immunoblot demonstrated significant PrP^{Sc} accumulation at 8 dpe (Fig. 2 H). In contrast, no replication was identified after exposure of VV astrocytes to an alternate sCJD prion strain from a patient with the less common VV1 subtype (Fig. 2 I). These findings highlight that specific factors associated with different prion strains, as well as genotypes, affect susceptibility to prion replication. To confirm that the susceptibility of MM astrocytes to vCJD prion infection was a function of their genotype and not caused by some unknown aspect of the specific iPSC1 MM cell line used, an additional independent MM astrocyte line (iPSC4) was tested, which again demonstrated serial accumulation of vCJD prions to levels beyond those present in the original inoculum (Fig. 2 J).

We next undertook quantitative immunocytochemistry to examine cellular accumulation of human prions in astrocytes after exposure to CJD prions. Immunocytochemistry was performed using guanidine (Gnd) pretreatment, which accentuates PrP^{Sc} staining by revealing cryptic epitopes buried in aggregated PrP^{Sc}. MM astrocytes exposed to vCJD (MM) inoculum and VV astrocytes exposed to sCJD (VV2) inoculum showed a significant increase in accumulation of PrP^{Sc} at 8 dpe (Fig. 3, A and D). In contrast, MV and VV astrocytes did not show an increase in PrP immunolabeling after exposure to vCJD

(MM) inoculum and had a similar appearance to unexposed control astrocyte cultures with faint punctate PrP^{C} immunolabeling (Fig. 3, B and C). Collectively, these data demonstrate that astrocytes are capable of replicating vCJD and sCJD prions; however, replication of vCJD prions over the first 8 d appeared constrained in part by the requirement of matching inoculum and cells for the *PRNP* codon 129 genotype.

Dose dependence and subpassage of human prions in naive astrocytes

To examine whether the apparent inability of MV and VV astrocytes to replicate vCJD prions was dose dependent, cultures of each genotype (MM, MV, and VV) were exposed to a range of vCJD inoculum doses from 0.1% to 5%. MM astrocytes showed clear dose-dependent replication of vCJD prions at 3 dpe. However, no evidence of prion replication was observed in either MV or VV astrocytes at 3 dpe (Fig. 4 A).

A key feature of prions is the ability to promote replication of PrP^{Sc} upon transmission to an uninfected host. To test whether PrP^{Sc} produced in human astrocytes was able to infect naive astrocyte culture, we next used extracts of astrocyte cultures that had previously been exposed to CJD brain homogenate and allowed to recover for 8 d as inoculum for naive (previously unexposed) astrocyte cultures. Exposure of naive MM astrocytes to vCJD-infected (MM) cell inoculum resulted in a substantially increased level of PrP^{Sc} compared with astrocytes during the first passage at 8 dpe (Fig. 4 B). A fourfold increase of PrP^{Sc} was also observed when VV naive astrocytes were exposed to a cell lysate from sCJD (VV2)–infected VV astrocytes (Fig. 4, C and D). Immunocytochemistry revealed aggregated PrP^{Sc} in infected cells compared with a faint PrP^{C} immunostain in unexposed control cells (Fig. 4 E). Both subpassage experiments demonstrate that vCJD and sCJD prions can be passed from CJD brain homogenate to a naive human astrocyte culture and further subpassaged, resulting in increased levels of PrP^{Sc}.

Figure 1. **Characteristics of iPSC–derived astroglial progenitor cells and astrocytes.** (A) Schematic representation of differentiation of healthy donor cells to astrocyte progenitors and astrocytes. (B) Representative immunographs and quantification of nestin and vimentin coexpression in APC cultures. (C) Representative immunographs of astrocytes of all lines immunostained for GFAP and GLAST from three replicate experiments. (D) A majority of cells of all lines are GFAP-expressing cells (iPSC1, 87.8 ± 1.7%; iPSC2, 91.4 ± 1.7%; and iPSC3, 89.2 ± 0.7%), with a minor proportion expressing the neuronal marker, NeuN (iPSC1, 6.3 ± 2%; iPSC2, 5.4 ± 1.8%; and iPSC3, 6 ± 0.4%). (E) Proliferating Ki67-positive cells in iPSC1, iPSC2, and iPSC3 APC and astrocyte cultures. (F) Functional evaluation of APC and astrocyte cultures by L-glutamate uptake assay. (G) Representative immunoblots of PrP^{C} expression in MM (iPSC1), MV (iPSC2), and VV (iPSC3) lines as APC cultures and their corresponding CNTF differentiated astrocytes from two samples each in two replicate experiments. The amount of total protein loaded was 20 µg/lane. The blots were developed with anti-PrP 3F4 antibody and then stripped and reprobed with anti–β actin antibody as a loading control. Molecular masses are in kilodaltons. (H) Maximum intensity projection of Z stacks of VV (iPSC3) astrocytes immunolabeled for PrP^{C} (green) and cell membrane (white) without and with Triton X-100 permeabilization. (I) Summary table of all cell lines and CJD strain combinations with their respective PRNP codon 129 polymorphisms used in this study. (J) Graphic representation of live/dead (viability/cytotoxicity) assay of iPSC1, iPSC2, and iPSC3 astrocytes exposed to 1% spin-filtered vCJD, sCJD, or NBHs for 24 h and analyzed immediately (0 dpe) or after 3 d of recovery in fresh media (3 dpe). Unexposed cells served as a baseline control for each cell line. Cell count of each group is represented as percentage of total cells, and the data were acquired from 10 randomized fields from three replicate experiments, unless otherwise stated. (B–F and J) Data are plotted as mean ± SEM and analyzed by one-way ANOVA, followed by Tukey's multicolumn comparison test; *, P < 0.05; ****, P < 0.0001; ns, not significant. (B, C, and H) Nuclei were stained with DAPI (blue). Bars, 20 µm.
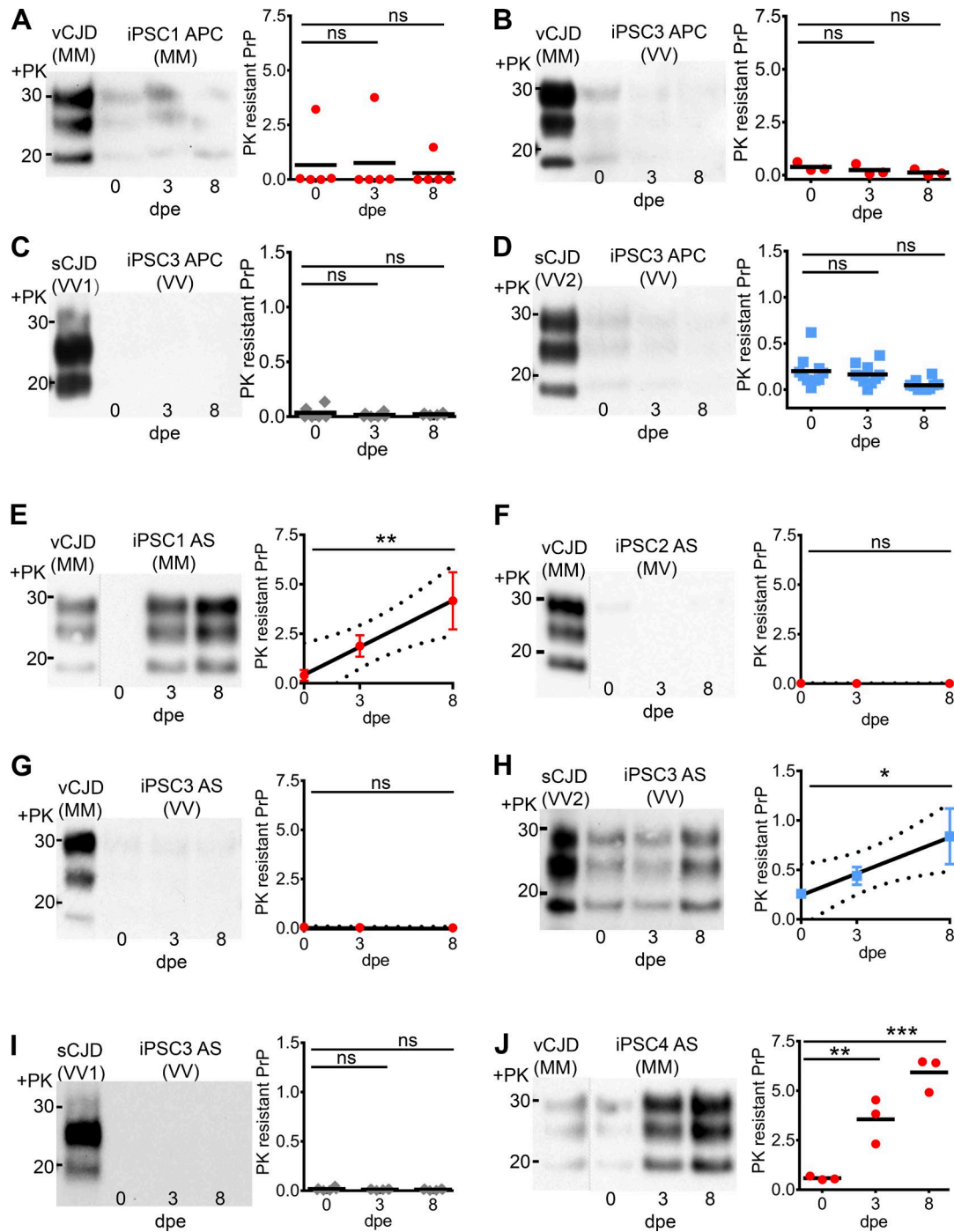
Figure 2. **Human iPSC–derived astrocytes replicate PrP^{Sc} in vitro in a PRNP codon 129–dependent manner.** APC and astrocyte cultures were analyzed by immunoblots immediately after 24 h of exposure (0 dpe), 3 and 8 dpe. (A) APC cultures of the MM (iPSC1) line exposed to 1% spin-filtered vCJD. APC cultures of the VV (iPSC3) line exposed to 1% spin-filtered vCJD (B), sCJD (VV1) (C), and sCJD (VV2) (D). (A–D) n = 1–3, in triplicate. (E) Astrocytes of the MM (iPSC1) genotype replicate PrP^{Sc} after exposure to 1% spin-filtered vCJD (MM) inoculum. (F) Astrocytes of MV (iPSC2) and (G) VV (iPSC3) genotypes exposed to 1% vCJD do not replicate PrP^{Sc}. (H) VV (iPSC3) astrocytes replicate PrP^{Sc} when exposed to 1% spin-filtered sCJD (VV2) brain homogenate. Representative immunoblots and linear regression of PK-resistant PrP^{Sc} level from n = 6 (E), n = 4 (F), n = 4 (G), and n = 4 (H) independent identical experiments generally performed in triplicate. (I) VV (iPSC3) astrocytes exposed to 1% spin-filtered sCJD (VV1) brain homogenate. (J) Independent MM (iPSC4) astrocytes exposed to 1% spin-filtered vCJD (MM). (I and J) n = 1–2, in triplicate. PK-resistant PrP^{Sc} signal values in cell lysates were normalized by the PrP^{Sc} signal value of the inoculum used in each individual experiment. A–D, I, and J are plotted including mean and analyzed by one-way ANOVA followed by Tukey's multicolumn comparison test. (E–H) Mean ± SEM. Linear regression was applied to establish a trend line (black) that is shown with 95% confidence bands (black dotted). Dashed gray lines in immunoblot images (E, F, and J) indicate a montage image in which lanes of the same blot and exposure have been rearranged for

Differing kinetics of vCJD and sCJD prion propagation in long-term astrocyte cultures

The recent identification of a vCJD case in a patient heterozygous at codon 129 of the *PRNP* (MV) with an extended incubation period compared with MM vCJD cases prompted us to explore whether the genotypic barriers previously observed in vitro can be overcome in longer-term experiments. We first tested MV astrocytes at time points 0, 8, 15, and 28 dpe to vCJD (MM). Although no PrP^{Sc} was evident up to 15 dpe, immunoblot at 28 dpe revealed PrP^{Sc} (Fig. 5 A). These findings suggest that heterozygous (MV) astrocytes are able to replicate vCJD prions from an MM genotype patient but that replication efficiency is very low when compared with vCJD (MM) prion replication in MM astrocytes (Fig. 2, E and J). We next exposed MM astrocytes to several different strains of human CJD prion disease inocula (vCJD MM, sCJD MM1, and sCJD VV2) and NBH as a control with assessment of PrP^{Sc} at time points up to 28 dpe (Fig. 5 B). Progressive accumulation of PrP^{Sc} was found in vCJD-treated MM astrocyte cultures (Fig. 5 B, lane 1). sCJD MM1 subtype brain homogenate displayed lower level PrP^{Sc} accumulation (Fig. 5 B, lane 2). PrP^{Sc} was also found in MM astrocyte cultures exposed to sCJD (VV2) brain homogenate at 28 dpe (Fig. 5 B, lane 3). No PrP^{Sc} could be observed in astrocytes exposed to control NBH (Fig. 5 B, lane 4). To further ascertain the impact of genotype on replication susceptibility and efficiency, we next exposed VV astrocytes to the sCJD (MM1) strain. VV astrocytes showed no detectable accumulation of PrP^{Sc} up to 28 dpe (Fig. 5 C). Finally, we exposed VV astrocytes to vCJD (MM), sCJD (VV1), or sCJD (VV2) subtypes for the same time periods. Consistent with earlier results, neither vCJD (MM) nor sCJD (VV1) prion strains showed detectable PrP^{Sc} replication in VV cells (Fig. 5 D, lanes 1 and 2); however, a very faint PrP^{Sc} signal was present at 28 dpe in VV astrocytes exposed to vCJD (Fig. 5 D, lane 1). VV astrocytes exposed to sCJD (VV2) showed abundant PrP^{Sc} accumulation over 28 d (Fig. 5 D, lane 3). In all cases of positive prion replication, the proteinase K (PK)–resistant PrP^{Sc} pattern showed identical mobility and glycoform ratio to those of the brain homogenate used for inocula, suggesting that the astrocyte cultures propagate strain-associated PrP^{Sc} conformers with biochemical fidelity (Fig. 2, E, H, and J; Fig. 4, B and C; and Fig. 5, A, B, and D).

Human prion replication in human stem cell–derived astrocytes

We report the first demonstration of human prion replication and prion strain kinetics in a physiologically relevant human cellular system. Specifically, we show that human iPSC–derived astrocytes efficiently replicate three distinct human prion strains (sCJD [MM1], sCJD [VV2], and vCJD [MM]), provided that genotypic barriers to replication and incubation period are respected. The inability of dividing APCs to support prion replication is in agreement with our previous study that proliferating undifferentiated human embryonic stem cells clear prions to subdetectable levels within 2–3 dpe (Krejciova et al., 2011). Our present findings using human iPSC–derived astrocytes are therefore consistent with the hypothesis that cellular susceptibility to prion infection is dependent on an appropriate CNS cellular phenotype.

Potential role of astrocytes in prion disease

Although astrocytes have long been known to be pivotal to maintaining CNS homeostasis, their role in neurodegenerative diseases has come to be appreciated only recently. This is not surprising given the intimate structural and functional association of astrocytes with, inter alia, the synapse and vasculature (Zuchero and Barres, 2015). Although astrocyte pathology is well described in prion disease, the role of astrocytes in prion pathobiology is unknown (Head et al., 2015). Experimental evidence from animal and cellular models supports the notion that astrocytes may have a role in prion propagation. These studies include the finding that PrP^{Sc} accumulation in astrocytes is an early event in scrapie pathogenesis, preceding overt neurodegeneration (Diedrich et al., 1991), as well as the observation that experimental scrapie pathology (including neuronal death) can occur in transgenic mice in which PrP^{C} expression is restricted to astrocytes (Raeber et al., 1997; Jeffrey et al., 2004; Kercher et al., 2004). These and other studies (Victoria et al., 2016) do not, however, distinguish between the possibility that astrocytic PrP^{Sc} is directly toxic to neurons and/or that PrP^{Sc} accumulated by astrocytes adversely affects the homeostatic/neuronal support role of astrocytes. The findings reported in this study establish an experimental platform that permits the study of cell-autonomous and non–cell autonomous consequences of astrocytic prion replication.

The role of *PRNP* codon 129 in vCJD prion replication

There have been 178 definite or probable cases of vCJD in the UK (1995–2017), and all tested cases have been MM, with the exception of a single vCJD case in a heterozygous patient (MV) who died in 2016, 16 yr after the first peak of cases in the MM genotype (Mok et al., 2017). One interpretation of this observation is that heterozygosity provides a substantial degree of protection from developing clinical vCJD, perhaps effected by limiting the rate of vCJD prion replication. Exposure of MM astrocyte cultures to vCJD inoculum resulted in a rapid and reproducible rise in PrP^{Sc}, first detected at 3 dpe, progressively continuing to the 28-d stage. In contrast, MV astrocyte cultures failed to accumulate detectable PrP^{Sc} at early time points, and

presentation purposes. Note: the y axis in all cells exposed to vCJD (A, B, E–G, and J) has a fivefold-extended range because of high levels of vCJD PrP^{Sc} accumulation detected in MM (iPSC1 and iPSC4) astrocytes. Blots were developed using anti-PrP 3F4 (A, E, F, and J) and HuM-P (B–D and G–I) antibodies. Molecular mass is indicated in kilodaltons. *, $P < 0.05$; **, $P < 0.01$; ***, $P < 0.001$; ns, not significant.
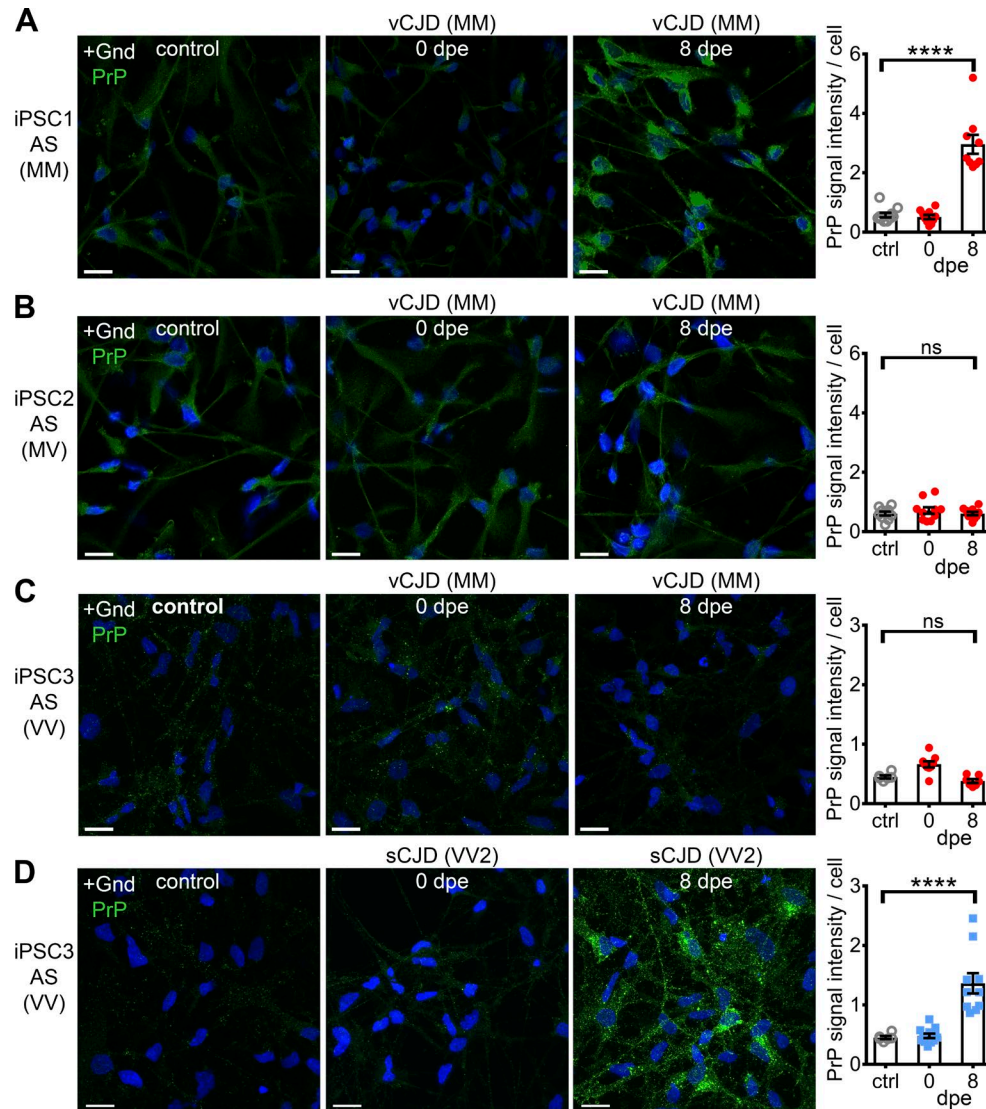
Figure 3. Human iPSC–derived astrocytes accumulate PrP^Sc when the CJD inoculum and cell PRNP codon 129 genotype are matched. (A) PrP^Sc accumulation in MM (iPSC1) astrocytes was observed at 8 dpe to 1% spin-filtered vCJD inoculum (bright green). Quantification of PrP immunolabeling intensity (right) showed significant increase in cell-associated PrP^Sc when compared with PrP^C of unexposed control cells. (B) MV (iPSC2) astrocytes fail to accumulate detectable PrP^Sc after exposure to 1% spin-filtered vCJD inoculum. Only the faint green immunolabeling of endogenous PrP^C can be seen. (C) VV (iPSC3) astrocytes fail to accumulate PrP^Sc when exposed to 1% spin-filtered vCJD. (D) PrP^Sc accumulation (bright green) in (iPSC3) VV astrocytes exposed to 1% spin-filtered sCJD (VV2) inoculum and allowed to recover for 8 d. Quantification of PrP immunolabeling intensity (right) showed significant increase in cell-associated PrP^Sc at 8 dpe. Faint green endogenous PrP^C signal is present in corresponding unexposed control cells in A–D. The data shown in A–D were generated from multiple fields from an experiment conducted in triplicate and are representative of experiments vCJD/iPSC1 ($n = 3$), vCJD/iPSC2 ($n = 2$), vCJD/iPSC3 ($n = 4$), and sCJD VV2/iPSC3 ($n = 7$). PrP signal was normalized by cell count. Data are plotted with mean ± SEM, analyzed by one-way ANOVA, and followed by Tukey's multicolumn comparison test: ****, $P < 0.0001$; ns, not significant. Cells were immunolabeled with anti-PrP antibody 6H4 (A and B) and HuM-P (C and D). Nuclei were stained with DAPI (blue). Bars, 20 µm. ctrl, control.

only at 28 dpe was a faint PrP^Sc signal observed. This implies that *PRNP* codon 129 genotypic effects on vCJD prion replication can be faithfully modeled in iPSC-derived astrocytes, and the results confirm that heterozygosity is an incomplete protective factor against vCJD (MM) prion replication in human populations, in transgenic modeling, in cellular, and in cell-free model systems (Bishop et al., 2006; Jones et al., 2009;

Mok et al., 2017). Furthermore, we demonstrate that genotype is also an important factor in prion replication in sCJD cases, whereby genotype-matched patient brain homogenate to the cellular genotype was more likely to result in efficient prion replication. An exception to this, however, was in the case of the sCJD (VV1) subtype, which did not efficiently replicate, even in cells of the VV genotype. This suggests that specific
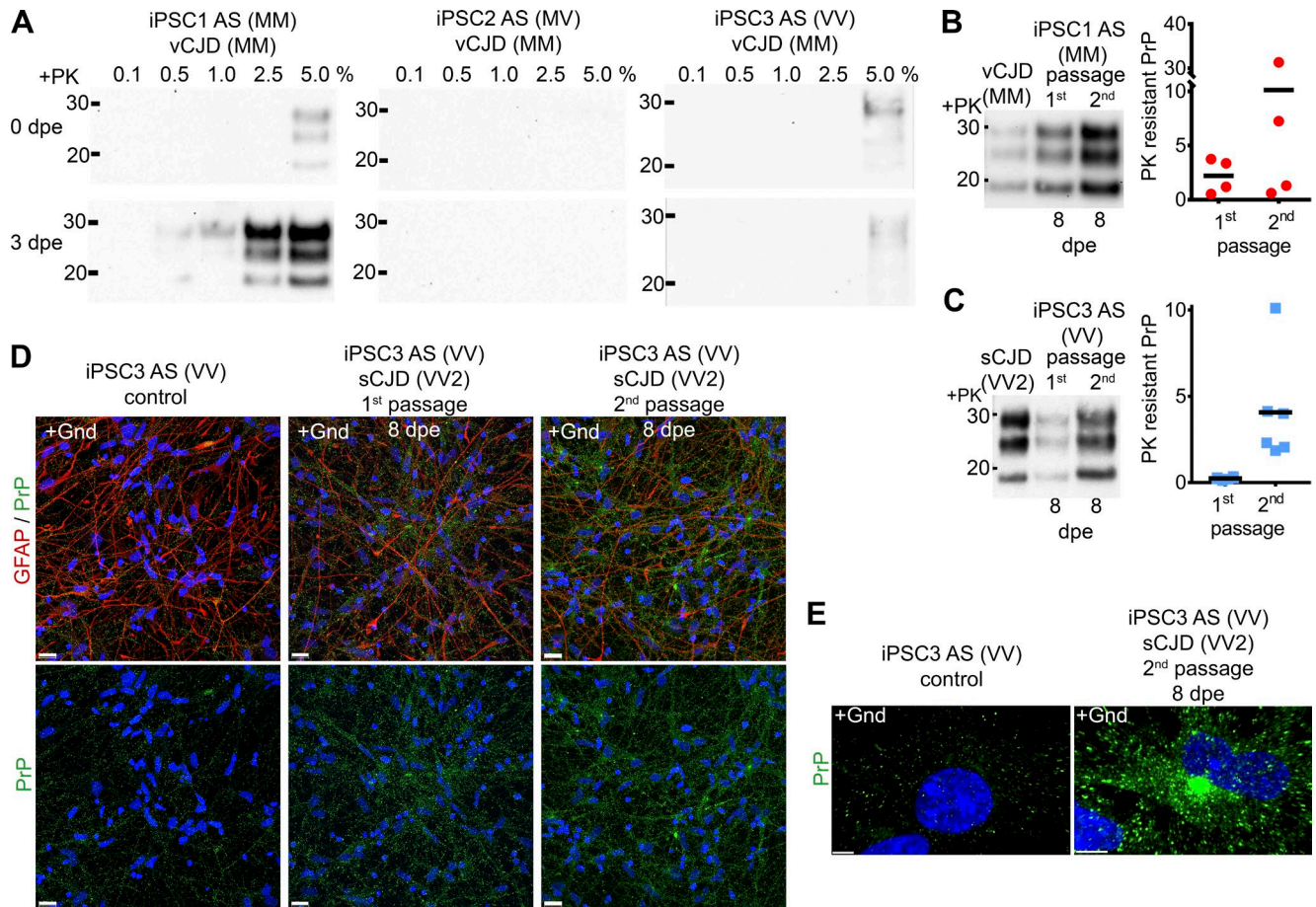
Figure 4. Dose–dependent accumulation and subpassage of CJD prions in iPSC–derived astrocytes. (A) Immunoblot analysis of astrocytes exposed to vCJD (MM) brain homogenate at five concentrations for 24 h and assayed immediately (0 dpe) or after recovery in fresh media for 3 d (3 dpe). MM (iPSC1) astrocytes replicate PrP^{Sc} in a concentration-dependent manner. MV (iPSC2) and VV (iPSC3) astrocytes failed to replicate PrP^{Sc} at 3 dpe. The experiment was conducted twice with similar results. (B) MM (iPSC1) astrocytes exposed to 1% spin-filtered vCJD brain homogenate. Both first and second passage were analyzed at 8 dpe. In the second passage experiment, the naive MM (iPSC1) astrocytes were exposed to vCJD-infected cell homogenate diluted to match PrP^{Sc} level of original vCJD brain homogenate used for exposure of astrocytes in the first passage. $n = 2$, in duplicate. (C) VV (iPSC3) astrocytes exposed to 1% spin-filtered sCJD (VV2) brain homogenate (first passage) and sCJD VV2–infected astrocyte homogenate (second passage). The naive VV (iPSC3) astrocytes were exposed to a whole sCJD-infected cell homogenate (1:1), i.e., cell lysate of a single well served as an inoculum for a new well because of a lower efficiency of sCJD prion propagation. Both passages were analyzed at 8 dpe. $n = 2$, in triplicate. Blots were developed using anti-PrP (A and B) 3F4 and (C) HuM-P antibodies. Molecular mass is indicated in kilodaltons. (B and C) Data are plotted with mean. PK-resistant PrP^{Sc} signal values in cell lysates were normalized by the PrP^{Sc} signal value of the inoculum used in each individual experiment. (D) Representative PrP and GFAP immunolabeling in VV (iPSC3) astrocytes exposed to 1% spin-filtered sCJD (VV2) brain homogenate (first passage, middle). VV astrocytes exposed to spin-filtered cell homogenate of astrocytes propagating sCJD (VV2; second passage, right). Both were analyzed at 8 dpe. PrP immunolabeling intensity (bright green) showed an increase in cell-associated PrP^{Sc} when astrocytes of first sCJD passage were compared with PrP^{C} of unexposed control cells (control, left), and PrP^{Sc} signal appeared more abundant in astrocytes in the second passage. $n = 2$, in triplicate. (E) Maximum intensity projection of Z stacks of VV (iPSC3) astrocytes immunolabeled for PrP at 8 dpe in cells exposed to sCJD (VV2) infected cell homogenate (right) and unexposed control (left). (D and E) Cells were immunolabeled with anti-PrP antibody 3F4. Nuclei were stained with DAPI (blue). Bars: (D) 20 µm; (E) 5 µm.

aspects of the prion strain itself might also play a substantial role in determining prion transmission, which is a comparable finding to earlier studies performed using transgenic mice expressing human PrP (Bishop et al., 2010).

Concluding remarks

To our knowledge, this study that utilizes human iPSC–derived astrocytes is the first to demonstrate that human cells of a relevant CNS phenotype are directly susceptible to infection with human prions. Importantly, our cell culture system effectively models known aspects of disease susceptibility, such as the high susceptibility of the *PRNP* codon 129 MM genotype to vCJD, as compared with the relative resistance of the MV or VV genotype. This work therefore represents a fundamental advance in modeling human prion disorders by establishing a readily scalable system with which to ad-
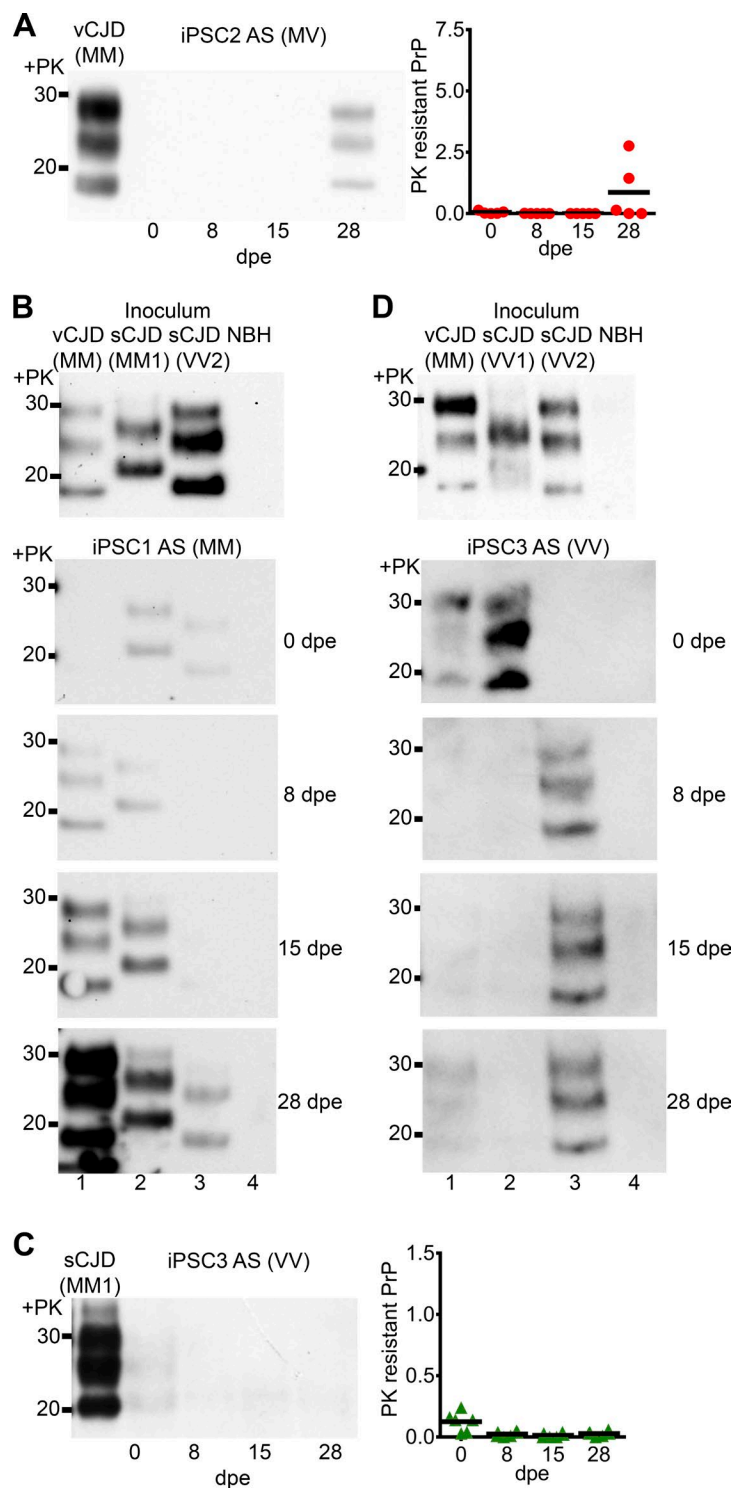
3488

Human prion propagation in human cell culture | Krejciova et al.

Figure 5. **Differing kinetics of vCJD and sCJD prion propagation in human iPSC–derived astrocytes.** In all experiments, astrocytes were exposed to 1% spin-filtered brain homogenate (24 h) and analyzed immediately (0 dpe) and at 8, 15, and 28 d later (8, 15, and 28 dpe). (A) Representative immunoblot of MV (iPSC2) astrocytes exposed to vCJD brain homogenate. Graphic representation of $n = 2$, duplicate and triplicate. (B) Immunoblots of MM (iPSC1) astrocytes exposed to 1% spin-filtered vCJD (lane 1), sCJD (MM1; lane 2), sCJD (VV2; lane 3), and NBH (lane 4). (C) Immunoblot of VV (iPSC3) astrocytes exposed to sCJD (MM1) brain homogenate. Representation of $n = 2$, in triplicate. (A and C) Data are plotted with mean. PK-resistant PrP^{Sc} signal values in cell lysates were normalized by the PrP^{Sc} signal value of the inoculum used in each individual experiment. (D) VV (iPSC3) astrocytes were exposed to vCJD (lane 1), sCJD (VV1; lane2), sCJD (VV2; lane 3), and NBH (lane 4). (B and D) Blots were developed at the same time/exposure; an example of $n = 3$ is shown. Blots were immunolabeled using anti-PrP 3F4 (A and B) and HuM-P (C and D) antibodies. Molecular mass is indicated in kilodaltons.

dress mechanistic aspects of human prion infection and to facilitate drug discovery.

MATERIALS AND METHODS

Human brain specimens and ethics statement

All human tissues in this study were handled in dedicated biosafety level 3* containment facilities according to stringent health and safety protocols at the University of Edinburgh and the University of California, San Francisco. Brain tissue from five cases of autopsy-proven vCJD were used interchangeably in this study. All vCJD cases were of UK origin and were referred to the National CJD Research & Surveillance Unit (NCJDRSU) for neuropathological diagnosis and surveillance purposes. A pathological diagnosis of vCJD had been made according to internationally accepted criteria (http://www. cjd.ed.ac.uk/sites/default/files/diagnostic%20criteria.pdf). The tissues were sampled from two female and three male patients who died at ages ranging from 19 to 53 between 1996 and 2003. Each was homozygous for methionine (MM) at the polymorphic codon 129 of the *PRNP* gene, and mutations in this gene were discounted by gene sequencing. Brain tissue from two of the five cases had previously been successfully used in experimental animal transmission studies. Brain tissue was also used from two cases of autopsy-proven sCJD: one of the MM1 subtype, a male who died at age 73 in 2003, and the other of the VV2 subtype, a male who died at age 53 in 1996. Both cases were of UK origin, referred to the NCJDRSU, and diagnosed according to internationally accepted criteria. Mutations in the *PRNP* sequence were excluded by gene sequencing. Brain tissue from the sCJD VV2 subtype case had previously been successfully used in experimental animal transmission studies. Brain tissue from a UK individual who had died suddenly of alcohol poisoning at age 24 in 2005, without neurological disease, and who was found to have no significant neuropathological abnormalities at autopsy examination, was used as a negative control for prion disease in some experiments reported here. These tissues from UK individuals were all provided to this study by request from the MRC Edinburgh Brain Bank under ethical approval from the East of Scotland Research Ethics Service REC 1 (reference number 16/ES/0084), with informed consent for research use provided by relatives of the deceased. Brain tissue from four further cases of sCJD were provided by the University of California, San Francisco Memory and Aging Center and were enrolled in the following research grants to M. Geschwind: R01AG031189 Early Diagnosis of Human Prion Diseases/Predicting Progression of Human Prion Diseases and P01AG021601 Novel Therapeutics for Prion Diseases. All tissues had consent for research use, provided by the relatives of the deceased. These sCJD cases comprised one case of the MM1 subtype (a female who died at age 66 in 2010), one case of the VV1 subtype (a female who died at age 53 in 2011), and two cases of the VV2 subtype (a female who died at age 62 in 2007 and a male who died at age 75 in 2012). Diagnoses were made in accordance with

internationally agreed criteria, and mutations in *PRNP* were excluded by gene sequencing. Brain tissue from the sCJD VV1 and one VV2 subtype case had previously been successfully used in experimental animal transmission studies. A further (prion disease negative) control brain used in this study, from a 63-yr-old male who died of a heart failure, was a gift to S.B. Prusiner (Institute for Neurodegenerative Disease, University of California, San Francisco, San Francisco, CA) from M. Ingelsson (Uppsala University, Uppsala, Sweden).

PRNP codon 129 genotype

DNA from all iPSC lines was isolated after cell lysis using the DNeasy blood and tissue kit (Qiagen). The codon 129 polymorphism of the *PRNP* gene (GenBank accession no. AL133396) was determined by restriction fragment length polymorphism analysis using NspI (New England Biolabs). In brief, the 956-bp *PRNP* gene sequence was PCR amplified using forward (5′-TGATACCATTGCTATGCACTC ATTC-3′) primer and reverse (5′-GACACCACCACTAAA AGGGCTGCAG-3′) primer at 5 pM each per reaction, 1× NEBuffer 1.1, 0.2 mM deoxynucleoside triphosphate (Promega), and 1 U of Taq polymerase (HotStarTaq; Qiagen). Restriction enzyme digestion was performed according to the manufacturer's instructions at 37°C. NspI cleaves the amplicon once at *PRNP* codon 155 and a second time at codon 129, only when the latter sequence codes for methionine (-ATG-). This enables distinction between the three *PRNP* codon 129 polymorphic genotypes MM, MV, and VV by agarose gel electrophoresis and Sybr green staining (Thermo Fisher Scientific).

iPSC lines and astrocyte differentiation

Previously generated iPSC-derived astrocyte precursors (APCs), shown to produce highly pure and functional astrocytes (Krencik and Zhang, 2011; Serio et al., 2013; Krencik et al., 2015) were designated iPSC1, iPSC2, and iPSC4 (34D6, Lord2R6, and 33D9, respectively; Serio et al., 2013) and iPSC3 (162D; Krencik and Zhang, 2011). APCs were grown in EGF/FGF-2 (R&D Systems)–containing media at 5 ng/ml each, as previously described (Krencik and Zhang, 2011), and tested negative for mycoplasma contamination. The protocol used for astrocyte differentiation had already been shown to yield cells that have astrocyte glutamate transporter function, and propagate calcium waves via extracellular ATP signaling and the cultures were lacking of neurons (Krencik et al., 2011). Moreover, there were no Iba1- or CD68-positive (macrophage) cells in the culture (Fig. 1 D and Fig. S1). Astrocytes differentiated using this protocol were shown to express a full range of astrocyte markers at the quantitative PCR and microarray levels and promote formation of synapses on human neurons (iPSC3 [162D]; Krencik et al., 2015). Astrocyte differentiation was as follows: APCs were dissociated with accutase (Stemcell Technologies), and then cells were plated on poly-L-ornithine (PLO; Sigma-Aldrich)– and matrigel (BD Matrigel Matrix Growth Factor Reduced; BD

Biosciences)-precoated wells. Cells were cultured in neurobasal media supplemented with 0.2% B27, 1% nonessential amino acids, 1% penicillin and streptomycin, 1% GlutaMax (all Gibco), and recombinant human ciliary CNTF (R&D Systems) at a final concentration of 10 ng/ml for 2 wk. Astrocyte cultures produced by this method were typically >90% pure when assessed by immunolabeling for the combination of astrocytic markers GLAST (Miltenyi Biotech) and GFAP (Millipore) and against the neuronal marker NeuN (Abcam), oligodendrocyte markers O4 (R&D Systems) and Olig2 (Chemicon), and macrophage markers Iba1 (Abcam) and CD68/SR-D1 (Novus).

Glutamate uptake assay

The method used to measure the decrease of glutamate in the media over time was adopted (Krencik et al., 2011). In brief, cells were plated on matrigel and cultured in EGF/FGF-2 (APC)– or CNTF (astrocyte; 10 ng/ml each)-containing media for 2 wk. Cells were dissociated with accutase and replated at equal density. 4 h after attachment, cells were pretreated with high sodium buffer for 30 min to equilibrate at 37°C (140 mM NaCl, 4 mM KCl, 2 mM MgCl$_2$, 1 mM CaCl$_2$, 23 mM glucose, and 15 mM Hepes, pH 7.4). Cells were then treated with high sodium buffer $\pm$ 500 µM L-glutamate for 1 h. Media was removed and L-glutamate concentration was determined using the glutamine/glutamate determination kit (Sigma-Aldrich). HEK293 cells, which do not significantly uptake glutamate when compared with differentiated astrocytes, were used as a baseline control. After subtraction of the blanks (no glutamate added), the decrease of glutamate in the media (or uptake by cells) was reported as micromolars of glutamate per microgram of protein after being normalized to the total protein in each well. The protein content was determined by a bicinchoninic acid protein assay (Pierce). Sample results were within range of a working standard curve. Values were normalized to cell numbers at the end of the assay. Values are reported as mean $\pm$ SEM.

Preparation of CJD inocula

Brain tissue was first homogenized at 10% weight to volume (wt/vol) in sterile phosphate buffered saline (PBS)/5% sucrose at 4°C and then ribolysed for 40 s (MP FastPrep-24). The homogenate was then sonicated (Sonicator 3000; Misonix) for 40 s at 80% power output and cleared of particulate matter by centrifugation at 424.1 g for 10 s at 4°C. The homogenate was then filtered by spin filters, pore size 220 nm (Agilent Technologies) or pore size 450 nm (Thermo Fisher Scientific), at 10,621 g for 15 min at 4°C. Cell homogenate inoculum was prepared by scraping astrocytes in Dulbecco's modified PBS (D-PBS) at 8 dpe to CJD brain homogenate. Cell homogenates were prepared as follows: astrocytes at 8 dpe to CJD brain homogenate were washed twice with ice-cold D-PBS, scraped in D-PBS using silicone cell scraper (USA Scientific), and homogenized using a 1-ml syringe with a 27-gauge needle, all at 4°C. Next the suspension was cleared

by centrifugation at 424.1 g for 10 s and spin filtered (pore size of 450 nm) at 4°C. Detection of PrP^{Sc} in the spin-filtered CJD brain homogenates and cell homogenates was confirmed by PK digestion (Novagen) at a final concentration of 50 µg/ml and immunoblot analysis.

Cell exposure regimen

APCs were plated at a density of 75,000 cells/well in 12-well plates precoated with PLO and matrigel and maintained in EGF/FGF-2–containing medium. Cells were plated at a lower density, in comparison to astrocytes, to accommodate the highly proliferative nature of APCs. APC cultures intended for astrocyte differentiation were plated at a density of 200,000 cells/well in 12-well plates precoated with PLO and matrigel and differentiated for 2 wk in CNTF-containing medium. Cells were exposed to vCJD, sCJD, or non-CJD brain homogenates (450 nm spin filtered and diluted in culture media) for 24 h. The medium was then discarded, and cells were washed twice with D-PBS at 37°C, given fresh (brain homogenate free) CNTF-containing medium, and further cultured. For time course studies, exposure was staggered according to the desired recovery time, and cultures were then harvested simultaneously, thus resulting in cultures of equivalent age in vitro. Exposure to human brain homogenate of individuals who died of a nonneurological cause (NBH) served as a negative control. Cells cultured exclusively in brain homogenate–free CNTF medium served as unexposed controls in all experiments. In subpassage experiments, naive astrocytes were exposed (24 h) to cell homogenate of astrocytes previously exposed to CJD brain homogenate and harvested at 8 dpe. Because of the differing prion replication efficiencies between cells of (MM or VV) *PRNP* polymorphism exposed to different prion strains, we chose to normalize the concentration of subpassaged cell homogenate (first passage) in two ways. First, lysate dilutions of MM (iPSC1) astrocytes exposed to vCJD were quantified for levels of PrP^{Sc} by immunoblots. The cell homogenate used for exposure was diluted to match the amount of PrP^{Sc} detected in the brain homogenate originally used to infect the astrocyte culture. However, in the case of iPSC3 (VV) astrocytes exposed to sCJD (VV2), a 1:1 well transmission of cell lysate to naive culture was performed instead because of the lower efficiency of sCJD prion replication. For immunocytochemistry experiments, APC plated on PLO and matrigel precoated glass coverslips (at a density of 50,000 cells/well in 24-well plates) were differentiated to astrocytes in CNTF media for 2 wk and then exposed to vCJD or sCJD brain homogenates (220 nm spin filtered and diluted in the CNTF medium) for 24 h. The conditions and procedures of each time course were as described above. Cultures from each time course experiment were terminated and immunolabeled at the same time and were therefore at the same culture stage.

Cell viability assay

The cytotoxic effect of the CJD and non-CJD NBH exposure was assessed by the LIVE/DEAD viability/cytotoxicity

assay (Thermo Fisher Scientific) according to the manufacturer's instructions. Unexposed cells served as a baseline control. Cells were viewed under a differential interference contrast microscope (CKX41; Olympus) with reflected fluorescence system 494-nm (green) and 528-nm (red) excitation filters. Captured images were analyzed using the particle counting plugin of ImageJ software (National Institutes of Health).

Anti–PrP antibodies

Immunoblotting for PrP used the mouse monoclonal antibody 3F4 obtained from Millipore (MAB1562, human PrP epitope 109–112) and the humanized Fab P (HuM-P, Prusiner Laboratory, human PrP epitope 96–105; Safar et al., 2002). Immunocytochemistry for PrP used the mouse monoclonal anti–PrP antibody 6H4 obtained from Prionics (01-010) or Thermo Fisher Scientific (7500997; human PrP epitope 144–152) and HuM-P. Each antibody recognizes an epitope in PrP^C that is retained in the protease-resistant core of PrP^{Sc}, and their specificity has been confirmed (Yull et al., 2006; Watts et al., 2014).

Immunoblot analysis

Immunoblotting for PrP followed the method of Krejciova et al. (2014a,b). In brief, each well was washed twice with 4°C D-PBS and then lysed on ice for 10 min with radio-immunoprecipitation assay extraction buffer (Sigma–Aldrich) containing protease inhibitors (Complete Mini EDTA-free; Roche) and EDTA at 5 mM. The lysate from each well was then collected using a silicone cell scraper into safe-lock tubes. The samples were digested with PK at a final concentration of 50 µg/ml at 37°C for 60 min, and digestion was terminated with 1 mM Pefablock SC (Roche). $MgCl_2$ and Benzonase at a final concentration of 1 mM and 50 U/ml, respectively, were added to the lysates and incubated at 37°C for 10 min before addition of 4× NuPAGE lithium dodecyl sulfate sample buffer (Novex) at a final concentration of 1×. The entire sample was then boiled at 100°C for 10 min and subjected to immunoblot analysis using antiprion protein monoclonal antibody 3F4 or HuM-P. The PK digestion step was omitted in immunoblotting experiments involving the detection of PrP^C/β–actin.

Immunocytochemistry

Immunocytochemistry followed the method of Krejciova et al. (2014b). In brief, cells were washed twice with D-PBS, fixed with 4% paraformaldehyde for 10 min, and permeabilized with 0.1% Triton X-100 for 10 min. A denaturation step involving Gnd thiocyanate (+Gnd) pretreatment during the immunolabeling procedure was necessary to retrieve PrP^{Sc} epitopes buried in nondenatured PrP^{Sc} aggregates (Giri et al., 2006). Cells were pretreated with 4 M Gnd for 10 min at room temperature (unless indicated otherwise, −Gnd) and blocked with 3% bovine serum albumin for 30 min. The cells were then incubated with the primary antibodies PrP antibody 6H4, 3F4, or HuM-P, anti-GFAP (Millipore), anti-

Nestin (Millipore), anti-Vimentin (Abcam), anti-NeuN, anti-Ki67 (Abcam), or anti-GLAST (Miltenyi Biotech), and subsequently the cells were incubated with the secondary antibodies Alexa Fluor 488 goat anti–mouse IgG1 antibody (Invitrogen) or goat anti–human IgG Fc F(ab′)2 FITC (Thermo Fisher Scientific), Alexa Fluor 555 goat anti–rabbit IgG (Invitrogen), and Alexa Fluor 647 goat anti–chicken IgG (Thermo Fisher Scientific). For plasma membrane staining experiments, CellMask (Molecular Probes) was applied to fixed cells for 10 min at 37°C before washing in PBS. The nuclei were counterstained with DAPI (Invitrogen). Slides were mounted with Vectashield (Vector Laboratories Ltd.) and examined by confocal microscopy using the LSM 710 (Zeiss) or TCS SP8 (Leica) microscope. All images from independent, but identical, experiments were acquired under the same conditions, and laser intensity levels were maintained constant throughout to reduce technical variability. Images were captured using the Zen 2012 black edition (Zeiss) or Las X (Leica) imaging software.

Image quantification and statistical analysis

For quantitative analysis of the cell viability assay, cells were counted from each time course over 10 randomly chosen areas, and the viable and nonviable cell counts were normalized to corresponding percentages of the cell population and plotted as a mean using Prism v.7 software (GraphPad). To assess the population of actively proliferating cells in the culture, APCs and astrocytes were immunolabeled for a cellular marker of proliferation, Ki67. DAPI counterstaining was used to assess total cell count in each culture. The count of proliferating cells was normalized by total cell count using the Prism v.7 software. Data were analyzed from two independent experiments ($n = 2$) in triplicate. Cell culture exposure and immunoblot analysis experiments were generally performed in triplicate (technical replicates) and repeated (experimental n) for each cell line, allowing for quantification and statistical analysis. No component parts of the reported experiments were excluded for presentational purposes. The numbers of independent identical experiments terminated at 8 dpe conducted for each cell line were APC cultures of iPSC1 ($n = 2$), iPSC3 ($n = 1$) for exposure to vCJD brain homogenate, and iPSC3 ($n = 2$ each) for exposure to sCJD VV1 and VV2. Astrocyte exposure was repeated as follows: iPSC1 ($n = 6$), iPSC2 ($n = 4$), iPSC3 ($n = 4$), iPSC4 ($n = 1$) for exposures to vCJD brain homogenate, and iPSC3 exposed to sCJD VV1 ($n = 2$) and VV2 ($n = 4$) brain homogenate. For the extended time point experiments up to 28 d, iPSC1 cells exposed to vCJD, sCJD MM1 or VV2, or a non-CJD brain homogenate ($n = 3$ each), iPSC2 astrocytes exposed to vCJD ($n = 2$), and iPSC3 exposed to vCJD, sCJD MM1, VV1 or VV2, or a non-CJD brain homogenate ($n = 2$ each). Astrocytes of the iPSC1 ($n = 2$) and iPSC3 ($n = 2$) were used in subpassage experiments. Densitometric analysis of the PK-resistant PrP^{Sc} bands detected by immunoblot was performed using the volume tool of the XRS+ System Image Lab 2.0 software (Bio-Rad). The

background signal values of individual blots were subtracted, and all samples were normalized against the PK–resistant PrP^{Sc} signal of the inoculum used in each individual experiment before data were analyzed and displayed using Prism v.7. Linear regression was applied to establish a trend line for the change in cell-associated protease–resistant PrP^{Sc} over time, which was normalized by the protease-resistant PrP^{Sc} signal in the inoculum to which the cell cultures were exposed.

The immunofluorescence data represent analysis of 9–12 images per time point per independent experiment. Each independent experiment was performed in triplicate, and the numbers of independent identical experiments conducted for each cell line were iPSC1 ($n = 3$), iPSC2 ($n = 2$), and iPSC3 ($n = 4$) for exposures to vCJD brain homogenate and iPSC3 ($n = 7$) exposed to sCJD (VV2) brain homogenate. Semiquantitative assessment was performed using the ImageJ histogram plugin to quantify the intensity of the green fluorescence of each image as described previously (Krejciova et al., 2014b). The green fluorescence pixel value (corresponding to PrP immunolabeling signal) was divided by the cell count of the analyzed image (corresponding to DAPI-stained nuclei), thus normalizing PrP immunolabeling to cell number. These values were plotted as arbitrary fluorescence units using Prism v.7 software, giving an intensity of PrP immunofluorescence per cell. Data were plotted with mean ± SEM and a one-way ANOVA followed by Tukey's multiple comparison test to determine variance compared with the control unexposed cells.

Online supplemental material
Fig. S1 demonstrates the presence of astrocytes after CNTF differentiation using the astrocyte marker GFAP and the absence of other CNS glial cells using the markers O4 and Olig2 for oligodendrocytes and Iba1 and CD68 for microglia.

REFERENCES
Alibhai, J., R.A. Blanco, M.A. Barria, P. Piccardo, B. Caughey, V.H. Perry, T.C. Freeman, and J.C. Manson. 2016. Distribution of misfolded prion protein seeding activity alone does not predict regions of neurodegeneration. *PLoS Biol.* 14:e1002579. https://doi.org/10.1371/journal.pbio.1002579

Arjona, A., L. Simarro, F. Islinger, N. Nishida, and L. Manuelidis. 2004. Two Creutzfeldt-Jakob disease agents reproduce prion protein-independent identities in cell cultures. *Proc. Natl. Acad. Sci. USA.* 101:8768–8773. https://doi.org/10.1073/pnas.0400158101

Asuni, A.A., B. Gray, J. Bailey, P. Skipp, V.H. Perry, and V. O'Connor. 2014. Analysis of the hippocampal proteome in ME7 prion disease reveals a predominant astrocytic signature and highlights the brain-restricted production of clusterin in chronic neurodegeneration. *J. Biol. Chem.* 289:4532–4545. https://doi.org/10.1074/jbc.M113.502690

Berry, D.B., D. Lu, M. Geva, J.C. Watts, S. Bhardwaj, A. Oehler, A.R. Renslo, S.J. DeArmond, S.B. Prusiner, and K. Giles. 2013. Drug resistance confounding prion therapeutics. *Proc. Natl. Acad. Sci. USA.* 110:E4160–E4169. https://doi.org/10.1073/pnas.1317164110

Bishop, M.T., P. Hart, L. Aitchison, H.N. Baybutt, C. Plinston, V. Thomson, N.L. Tuzi, M.W. Head, J.W. Ironside, R.G. Will, and J.C. Manson. 2006. Predicting susceptibility and incubation time of human-to-human transmission of vCJD. *Lancet Neurol.* 5:393–398. https://doi.org/10.1016/S1474-4422(06)70413-6

Bishop, M.T., R.G. Will, and J.C. Manson. 2010. Defining sporadic Creutzfeldt-Jakob disease strains and their transmission properties. *Proc. Natl. Acad. Sci. USA.* 107:12005–12010. https://doi.org/10.1073/pnas.1004688107

Cronier, S., V. Beringue, A. Bellon, J.M. Peyrin, and H. Laude. 2007. Prion strain- and species-dependent effects of antiprion molecules in primary neuronal cultures. *J. Virol.* 81:13794–13800. https://doi.org/10.1128/JVI.01502-07

Cunningham, C., R. Deacon, H. Wells, D. Boche, S. Waters, C.P. Diniz, H. Scott, J.N. Rawlins, and V.H. Perry. 2003. Synaptic changes characterize early behavioural signs in the ME7 model of murine prion disease. *Eur. J. Neurosci.* 17:2147–2155. https://doi.org/10.1046/j.1460-9568.2003.02662.x

Deleault, N.R., D.J. Walsh, J.R. Piro, F. Wang, X. Wang, J. Ma, J.R. Rees, and S. Supattapone. 2012. Cofactor molecules maintain infectious conformation and restrict strain properties in purified prions. *Proc. Natl. Acad. Sci. USA.* 109:E1938–E1946. https://doi.org/10.1073/pnas.1206999109

Diedrich, J.F., P.E. Bendheim, Y.S. Kim, R.I. Carp, and A.T. Haase. 1991. Scrapie-associated prion protein accumulates in astrocytes during scrapie infection. *Proc. Natl. Acad. Sci. USA.* 88:375–379. https://doi.org/10.1073/pnas.88.2.375

Giles, K., D.B. Berry, C. Condello, R.C. Hawley, A. Gallardo-Godoy, C. Bryant, A. Oehler, M. Elepano, S. Bhardwaj, S. Patel, et al. 2015. Different 2-aminothiazol therapeutics produce distinct patterns of scrapie prion neuropathology in mouse brains. *J. Pharmacol. Exp. Ther.* 355:2–12. https://doi.org/10.1124/jpet.115.224659

Giri, R.K., R. Young, R. Pitstick, S.J. DeArmond, S.B. Prusiner, and G.A. Carlson. 2006. Prion infection of mouse neurospheres. *Proc. Natl. Acad. Sci. USA.* 103:3875–3880. https://doi.org/10.1073/pnas.0510902103

Gómez-Nicola, D., N.L. Fransen, S. Suzzi, and V.H. Perry. 2013. Regulation of microglial proliferation during chronic neurodegeneration. *J. Neurosci.* 33:2481–2493. https://doi.org/10.1523/JNEUROSCI.4440-12.2013

Grassmann, A., H. Wolf, J. Hofmann, J. Graham, and I. Vorberg. 2013. Cellular aspects of prion replication in vitro. *Viruses.* 5:374–405. https://doi.org/10.3390/v5010374

Gray, B.C., Z. Siskova, V.H. Perry, and V. O'Connor. 2009. Selective presynaptic degeneration in the synaptopathy associated with ME7-induced hippocampal pathology. *Neurobiol. Dis.* 35:63–74. https://doi.org/10.1016/j.nbd.2009.04.001

Hannaoui, S., A. Gougerot, N. Privat, E. Levavasseur, N. Bizat, J.J. Hauw, J.P. Brandel, and S. Haïk. 2014. Cycline efficacy on the propagation of human prions in primary cultured neurons is strain-specific. *J. Infect. Dis.* 209:1144–1148. https://doi.org/10.1093/infdis/jit623

Head, M.W., J.W. Ironside, B. Ghetti, M. Jeffrey, P. Piccardo, and R.G. Will. 2015. Prion diseases. *In* Greenfield's Neuropathology. Ninth edition. S. Love, A. Perry, J. Ironside, and H. Budka, editors. CRC Press, Boca Raton, FL. 1016–1086.

Hennessy, E., E.W. Griffin, and C. Cunningham. 2015. Astrocytes are primed by chronic neurodegeneration to produce exaggerated chemokine and cell infiltration responses to acute stimulation with the cytokines IL-1β and TNF-α. *J. Neurosci.* 35:8411–8422. https://doi.org/10.1523/JNEUROSCI.2745-14.2015

Jeffrey, M., C.M. Goodsir, R.E. Race, and B. Chesebro. 2004. Scrapie-specific neuronal lesions are independent of neuronal PrP expression. *Ann. Neurol.* 55:781–792. https://doi.org/10.1002/ana.20093

Jones, M., D. Wight, R. Barron, M. Jeffrey, J. Manson, C. Prowse, J.W. Ironside, and M.W. Head. 2009. Molecular model of prion transmission to humans. *Emerg. Infect. Dis.* 15:2013–2016. https://doi.org/10.3201/eid1512.090194

Jones, M., A.H. Peden, M.W. Head, and J.W. Ironside. 2011. The application of in vitro cell-free conversion systems to human prion diseases. *Acta Neuropathol.* 121:135–143. https://doi.org/10.1007/s00401-010-0708-8

Kercher, L., C. Favara, C.C. Chan, R. Race, and B. Chesebro. 2004. Differences in scrapie-induced pathology of the retina and brain in transgenic mice that express hamster prion protein in neurons, astrocytes, or multiple cell types. *Am. J. Pathol.* 165:2055–2067. https://doi.org/10.1016/S0002-9440(10)63256-7

Krejciova, Z., S. Pells, E. Cancellotti, P. Freile, M. Bishop, K. Samuel, G.R. Barclay, J.W. Ironside, J.C. Manson, M.L. Turner, et al. 2011. Human embryonic stem cells rapidly take up and then clear exogenous human and animal prions in vitro. *J. Pathol.* 223:635–645. https://doi.org/10.1002/path.2832

Krejciova, Z., M.A. Barria, M. Jones, J.W. Ironside, M. Jeffrey, L. González, and M.W. Head. 2014a. Genotype-dependent molecular evolution of sheep bovine spongiform encephalopathy (BSE) prions in vitro affects their zoonotic potential. *J. Biol. Chem.* 289:26075–26088. https://doi.org/10.1074/jbc.M114.582965

Krejciova, Z., P. De Sousa, J. Manson, J.W. Ironside, and M.W. Head. 2014b. Human tonsil-derived follicular dendritic-like cells are refractory to human prion infection in vitro and traffic disease-associated prion protein to lysosomes. *Am. J. Pathol.* 184:64–70. https://doi.org/10.1016/j.ajpath.2013.09.013

Krencik, R., and S.C. Zhang. 2011. Directed differentiation of functional astroglial subtypes from human pluripotent stem cells. *Nat. Protoc.* 6:1710–1717. https://doi.org/10.1038/nprot.2011.405

Krencik, R., J.P. Weick, Y. Liu, Z.J. Zhang, and S.C. Zhang. 2011. Specification of transplantable astroglial subtypes from human pluripotent stem cells. *Nat. Biotechnol.* 29:528–534. https://doi.org/10.1038/nbt.1877

Krencik, R., K.C. Hokanson, A.R. Narayan, J. Dvornik, G.E. Rooney, K.A. Rauen, L.A. Weiss, D.H. Rowitch, and E.M. Ullian. 2015. Dysregulation of astrocyte extracellular signaling in Costello syndrome. *Sci. Transl. Med.* 7:286ra66. https://doi.org/10.1126/scitranslmed.aaa5645

Ladogana, A., Q. Liu, Y.G. Xi, and M. Pocchiari. 1995. Proteinase-resistant protein in human neuroblastoma cells infected with brain material from Creutzfeldt-Jakob patient. *Lancet.* 345:594–595. https://doi.org/10.1016/S0140-6736(95)90508-1

Lawson, V.A., L.J. Vella, J.D. Stewart, R.A. Sharples, H. Klemm, D.M. Machalek, C.L. Masters, R. Cappai, S.J. Collins, and A.F. Hill. 2008. Mouse-adapted sporadic human Creutzfeldt-Jakob disease prions propagate in cell culture. *Int. J. Biochem. Cell Biol.* 40:2793–2801. https://doi.org/10.1016/j.biocel.2008.05.024

Liddelow, S.A., K.A. Guttenplan, L.E. Clarke, F.C. Bennett, C.J. Bohlen, L. Schirmer, M.L. Bennett, A.E. Münch, W.S. Chung, T.C. Peterson, et al. 2017. Neurotoxic reactive astrocytes are induced by activated microglia. *Nature.* 541:481–487. https://doi.org/10.1038/nature21029

McCutcheon, S., A.R. Alejo Blanco, E.F. Houston, C. de Wolf, B.C. Tan, A. Smith, M.H. Groschup, N. Hunter, V.S. Hornsey, I.R. MacGregor, et al. 2011. All clinically-relevant blood components transmit prion disease following a single blood transfusion: a sheep model of vCJD. *PLoS One.* 6:e23169. https://doi.org/10.1371/journal.pone.0023169

Mok, T., Z. Jaunmuktane, S. Joiner, T. Campbell, C. Morgan, B. Wakerley, F. Golestani, P. Rudge, S. Mead, H.R. Jäger, et al. 2017. Variant Creutzfeldt-Jakob disease in a patient with heterozygosity at PRNP codon 129. *N. Engl. J. Med.* 376:292–294. https://doi.org/10.1056/NEJMc1610003

Parchi, P., A. Giese, S. Capellari, P. Brown, W. Schulz-Schaeffer, O. Windl, I. Zerr, H. Budka, N. Kopp, P. Piccardo, et al. 1999. Classification of sporadic Creutzfeldt-Jakob disease based on molecular and phenotypic analysis of 300 subjects. *Ann. Neurol.* 46:224–233. https://doi.org/10.1002/1531-8249(199908)46:2<224::AID-ANA12>3.0.CO;2-W

Parchi, P., R. Strammiello, S. Notari, A. Giese, J.P. Langeveld, A. Ladogana, I. Zerr, F. Roncaroli, P. Cras, B. Ghetti, et al. 2009. Incidence and spectrum of sporadic Creutzfeldt-Jakob disease variants with mixed phenotype and co-occurrence of PrPSc types: an updated classification. *Acta Neuropathol.* 118:659–671. https://doi.org/10.1007/s00401-009-0585-1

Prusiner, S.B. 2013. Biology and genetics of prions causing neurodegeneration. *Annu. Rev. Genet.* 47:601–623. https://doi.org/10.1146/annurev-genet-110711-155524

Raeber, A.J., R.E. Race, S. Brandner, S.A. Priola, A. Sailer, R.A. Bessen, L. Mucke, J. Manson, A. Aguzzi, M.B. Oldstone, et al. 1997. Astrocyte-specific expression of hamster prion protein (PrP) renders PrP knockout mice susceptible to hamster scrapie. *EMBO J.* 16:6057–6065. https://doi.org/10.1093/emboj/16.20.6057

Safar, J.G., M. Scott, J. Monaghan, C. Deering, S. Didorenko, J. Vergara, H. Ball, G. Legname, E. Leclerc, L. Solforosi, et al. 2002. Measuring prions causing bovine spongiform encephalopathy or chronic wasting disease by immunoassays and transgenic mice. *Nat. Biotechnol.* 20:1147–1150. https://doi.org/10.1038/nbt748

Serio, A., B. Bilican, S.J. Barmada, D.M. Ando, C. Zhao, R. Siller, K. Burr, G. Haghi, D. Story, A.L. Nishimura, et al. 2013. Astrocyte pathology and the absence of non-cell autonomy in an induced pluripotent stem cell model of TDP-43 proteinopathy. *Proc. Natl. Acad. Sci. USA.* 110:4697–4702. https://doi.org/10.1073/pnas.1300398110

Stahl, N., D.R. Borchelt, K. Hsiao, and S.B. Prusiner. 1987. Scrapie prion protein contains a phosphatidylinositol glycolipid. *Cell.* 51:229–240. https://doi.org/10.1016/0092-8674(87)90150-4

Stewart, L.A., L.H.M. Rydzewska, G.F. Keogh, and R.S.G. Knight. 2008. Systematic review of therapeutic interventions in human prion disease. *Neurology.* 70:1272–1281. https://doi.org/10.1212/01.wnl.0000308955.25760.c2

3494

Human prion propagation in human cell culture | Krejciova et al.

Trevitt, C.R., and J. Collinge. 2006. A systematic review of prion therapeutics in experimental models. *Brain*. 129:2241–2265. https://doi.org/10.1093/brain/awl150

Victoria, G.S., A. Arkhipenko, S. Zhu, S. Syan, and C. Zurzolo. 2016. Astrocyte-to-neuron intercellular prion transfer is mediated by cell-cell contact. *Sci. Rep.* 6:20762. https://doi.org/10.1038/srep20762

Wang, F., X. Wang, C.G. Yuan, and J. Ma. 2010. Generating a prion with bacterially expressed recombinant prion protein. *Science.* 327:1132–1135. https://doi.org/10.1126/science.1183748

Watts, J.C., and S.B. Prusiner. 2014. Mouse models for studying the formation and propagation of prions. *J. Biol. Chem.* 289:19841–19849. https://doi.org/10.1074/jbc.R114.550707

Watts, J.C., K. Giles, S. Patel, A. Oehler, S.J. DeArmond, and S.B. Prusiner. 2014. Evidence that bank vole PrP is a universal acceptor for prions. *PLoS Pathog.* 10:e1003990. https://doi.org/10.1371/journal.ppat.1003990

Yull, H.M., D.L. Ritchie, J.P.M. Langeveld, F.G. van Zijderveld, M.E. Bruce, J.W. Ironside, and M.W. Head. 2006. Detection of type 1 prion protein in variant Creutzfeldt-Jakob disease. *Am. J. Pathol.* 168:151–157. https://doi.org/10.2353/ajpath.2006.050766

Zuchero, J.B., and B.A. Barres. 2015. Glia in mammalian development and disease. *Development*. 142:3805–3809. https://doi.org/10.1242/dev.129304